Penta-1,2,3,4,6-*O*-galloyl-β-D-glucose induces p53 and inhibits STAT3 in prostate cancer cells *in vitro* and suppresses prostate xenograft tumor growth *in vivo*

Hongbo Hu,[1] Hyo-Jeong Lee,[1,2] Cheng Jiang,[1] Jinhui Zhang,[1] Lei Wang,[1] Yan Zhao,[1] Qiu Xiang,[1] Eun-Ok Lee,[2] Sung-Hoon Kim,[1,2] and Junxuan Lü[1]

[1]The Hormel Institute, University of Minnesota, Austin, Minnesota and [2]Cancer Preventive Material Development Research Center and Institute, College of Oriental Medicine, Kyunghee University, Seoul, Republic of Korea

Abstract

Penta-1,2,3,4,6-*O*-galloyl-β-D-glucose (PGG) is a naturally occurring gallotannin from some Oriental herbs. Several cell culture studies suggested a potential for PGG as a novel agent for the chemoprevention and treatment of cancer. Here, we investigated the cell death signaling mechanisms induced by PGG in human prostate cancer cells of different p53 functional status. We observed the induction of G_1- and S-phase arrests and caspase-mediated apoptosis in the androgen-dependent human LNCaP cells, which express wild-type p53, and in the androgen-independent, p53-mutant DU145 cells. In LNCaP cells, caspase-mediated apoptosis induction by PGG was associated with and mediated in major part by activation of p53 as established through small interfering RNA knockdown and dominant-negative mutant approaches. Intracellular reactive oxygen species production by PGG was found to be crucial for these molecular and cellular actions. In DU145 cells, which harbor constitutively active signal transducer and activator of transcription 3 (STAT3), caspase-mediated apoptosis induction by PGG was associated with an inhibition of STAT3 Tyr^{705} phosphorylation and the down-regulation of STAT3 transcriptional targets Bcl-XL and Mcl-1. Overexpression of Bcl-XL or knockdown of its binding partner Bak attenuated apoptosis induction. Furthermore, we provide, for the first time, *in vivo* data that PGG significantly inhibited DU145 xenograft growth in an athymic nude mouse model in association with an inhibition of pSTAT3. Our data support PGG as a multi-targeting agent for chemoprevention and therapy of prostate cancer by activating the p53 tumor suppressor pathway and by inhibiting STAT3 oncogenic signaling. [Mol Cancer Ther 2008;7(9):2681–91]

Introduction

Prostate cancer is the most commonly diagnosed cancer that affects one in six American men (1). Notable features of prostate cancer that make chemoprevention a rational and cost-effective approach include its ubiquity and its long latency between premalignant lesions and clinically evident cancers (2). The induction of tumor suppressor signaling such as the p53 axis (3) and/or an inhibition of oncogenic signaling such as signal transducer and activator of transcription 3 (STAT3; refs. 4, 5) in precancerous or cancer cells could be potential molecular mechanisms of prostate cancer primary or secondary chemoprevention.

p53 is the first identified and the best known tumor suppressor that controls cell cycle checkpoints and apoptosis and DNA repair (6). p53 is mutated in over half of all human tumors (7). Activation of p53 signaling through transcriptional and post-transcriptional modifications such as phosphorylation could be an effective approach against precancerous and cancer cells bearing the wild-type p53. Therefore, p53 is considered to be a rational molecular target not only for cancer therapy but also for chemoprevention. Indeed, several phytochemical cancer chemopreventive agents such as epigallocatechin-3-gallate (8), resveratrol (9), and curcumin (10), have been reported to induce apoptosis through the p53-dependent signaling pathway.

In contrast to normal cells, the transformed cells can become ''oncogene addicted.'' STAT proteins, identified originally as key components of cytokine signaling pathways, are a family of latent cytoplasmic transcription factors that act downstream of Janus-activated kinase or Src kinase activation and mediate intracellular signaling from a wide variety of cytokines, growth factors, and hormones (11, 12). Constitutive activation of STAT3 and other family members has been detected in a wide variety of human tumor specimens and cancer cell lines, including prostate cancer (12). STAT3 is activated by phosphorylation at Tyr^{705}, which induces dimerization, nuclear translocation, and DNA binding (13). Transcriptional activation activity of STAT3 is further regulated by phosphorylation at Ser^{727}. Key downstream targets of STAT3 include cyclin D1 for cell cycle regulation, Bcl-XL, and the related Mcl-1 for cell survival (14). It has been

Received 5/9/08; revised 6/13/08; accepted 6/15/08.

Grant support: The Hormel Foundation, The Prostate Cancer Foundation, NIH grant CA95642, and MCR grant R13-2007-019-00000-0 from Korea Ministry of Education, Science and Technology.

The costs of publication of this article were defrayed in part by the payment of page charges. This article must therefore be hereby marked *advertisement* in accordance with 18 U.S.C. Section 1734 solely to indicate this fact.

Requests for reprints: Junxuan Lü, The Hormel Institute, University of Minnesota, 801 16th Avenue Northeast, Austin, MN 55912, Phone: 507-437-9680; Fax: 507-437-9606. E-mail: jlu@hi.umn.edu

doi:10.1158/1535-7163.MCT-08-0456

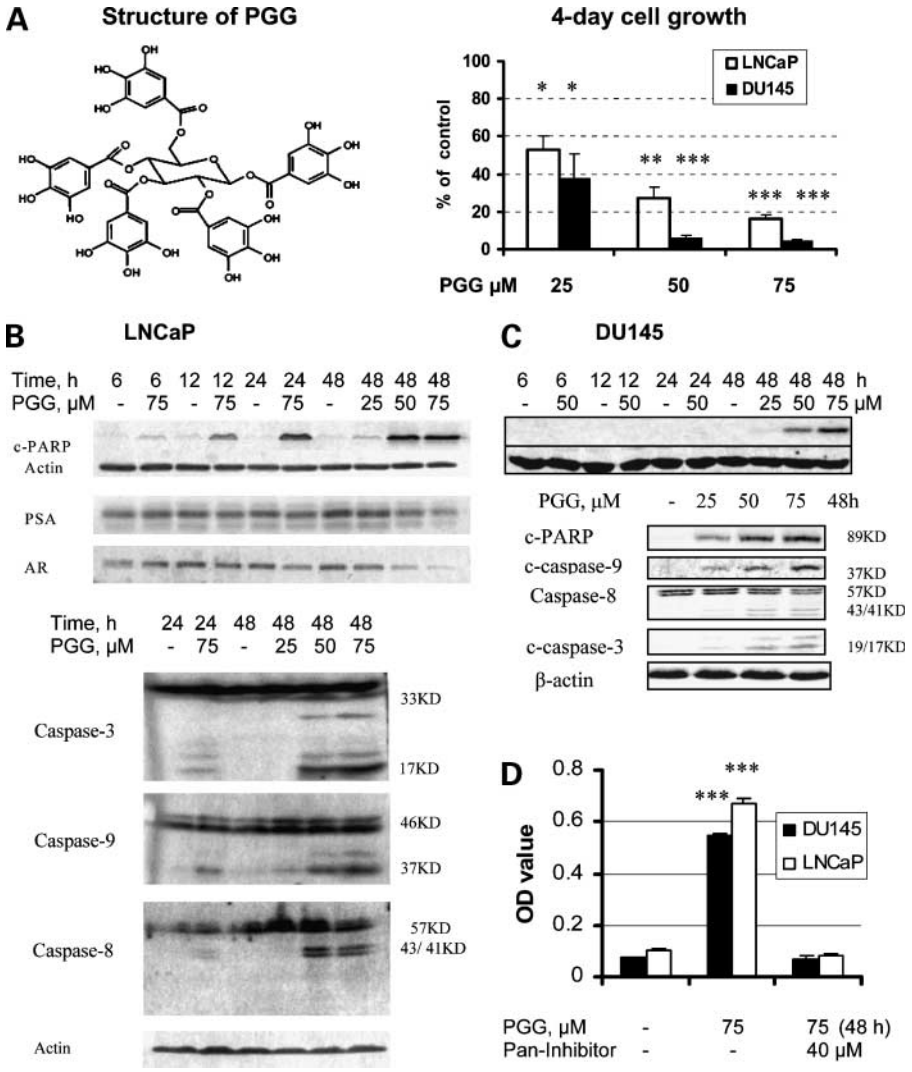

Figure 1. PGG induces caspase-mediated apoptosis in androgen-dependent and androgen-independent prostate cancer cells. **A,** chemical structure of PGG and overall inhibitory effects on LNCaP and DU145 cell number after 4 d of daily treatment. After treatments, cells were fixed with glutaraldehyde and stained with 0.02% aqueous solution of crystal violet. The stained cells were solublized with 70% ethanol and the absorbance was evaluated using a plate reader. Expressed as percentage of control cell set as 100. *, $P < 0.05$; **, $P < 0.01$; ***, $P < 0.001$, compared with respective control ($n = 3$ wells of 6-well plates). **B,** Western blot analysis of androgen receptor and PSA expression and cleavage of PARP and caspases in PGG-treated LNCaP cells. **C,** Western blot analysis of cleavage of PARP and caspases in PGG-treated DU145 cells. **D,** effects of a pan-caspase inhibitor on PGG-induced apoptosis in LNCaP and DU145 cells. Apoptosis was estimated by death ELISA assay after 48 h treatment with PGG and/or pan-caspase inhibitor. ***, $P < 0.001$, compared with PGG treatment alone ($n = 4$).

shown that, in DU145 cells, which have constitutively active STAT3 (15), inhibition of STAT3 signaling by small interfering RNA (siRNA) or other genetic approaches was sufficient to induce caspase-mediated apoptosis (16, 17). Interleukin-6 (IL-6) is a multifunctional cytokine that regulates the growth and differentiation of many cancers. Elevated expression of IL-6 has been implicated in prostate cancer androgen-independent progression, neuroendocrine differentiation, and drug resistance, which are associated with activation of STAT3 (18–20). Compounds that inhibit STAT3 signaling may therefore be good candidates for chemoprevention of prostate cancer (4).

Polyphenolic compounds are among the various chemopreventive agents that have shown promise for inhibiting prostate cancer carcinogenesis in pre-clinical models (21). Penta-1,2,3,4,6-*O*-galloyl-β-D-glucose (PGG; Fig. 1A) is a naturally occurring gallotannin polyphenolic compound in Oriental herbs such as *Galla rhois*, the gallnut of *Rhus chinensis* Mill, and the root of peony *Paeonia suffruticosa* Andrews. Several cell culture studies with prostate cancer cells and other cancer cell lines have shown multibiological activities of PGG that confer potential chemopreventive effect. For example, PGG inhibited growth of LNCaP prostate cancer cells and the secretion of androgen-regulated gene product, prostate-specific antigen (PSA; ref. 22). In the test tube, PGG was shown to inhibit rat liver microsomal 5α-reductase activity, which converts testosterone to the more active dihydrotestosterone (22). Such results suggest a potential efficacy of PGG to inhibit the androgen-dependent growth of prostate cancer. In addition to prostate cancer cells, PGG was shown to induce apoptosis of leukemia and breast cancer cells (23) and estrogen receptor signaling (24). PGG also was reported to inhibit invasion-related molecules such as matrix metalloproteinase-9 in melanoma cells (25). A recent study by coauthor Kim's group (26) has revealed that PGG possesses potent antiangiogenic

and proapoptotic activities and exerts a strong *in vivo* antitumor growth effect in a mouse Lewis lung cancer (LLC) allograft model. The signaling mechanisms for these biological effects of PGG still remain poorly defined, although a few *in vitro* studies showed that it may inhibit activator protein-1 activity in melanoma cells (25), nuclear factor-κB activity in macrophages (27), and cyclooxygenase-2 activities in vascular endothelial cells (26). Although these reported *in vitro* and *in vivo* effects suggest a probable anticancer activity of PGG against prostate cancer, its *in vivo* efficacy has not been established to date.

In this report, we investigated the effects of PGG on p53 and STAT3 signaling in apoptosis induction and established for the first time *in vivo* efficacy of PGG to inhibit DU145 prostate cancer xenograft growth in an athymic nude mouse model. Our data support the hypothesis that PGG may be an *in vivo* active prostate cancer chemopreventive agent by targeting multiple critical molecular and cellular pathways.

Materials and Methods

Chemicals and Reagents

PGG (molecular weight = 986) was isolated from *G. rhois*, the gallnut of *R. chinensis* Mill (26). The purity was ~98%. The general caspase inhibitor (zVADfmk) was purchased from MP Biomedicals. Antibodies specific for phospho-p53 Ser^{15}, Bax, $p21^{CiP1}$, Bcl-XL, Mcl-1, cleaved poly(ADP-ribose) polymerase (PARP; p89), caspase-3, -8, and -9, cleaved caspase-3 and -9 and phospho-STAT3 were purchased from Cell Signaling Technology. An antibody for cyclin D1 was purchased from Santa Cruz Biotechnologies. *N*-acetyl-L-cysteine and an antibody for β-actin were purchased from Sigma. Hydroethidine and 6-carboxy-2′,7′-dichlorodihydrofluorescein diacetate were purchased from Molecular Probes. Manganese(III) tetrakis(*N*-methyl-2-pyridyl)porphyrin, a superoxide dismutase mimetic chemical, was purchased from Alexis Biochemicals.

Cell Culture and Treatments

LNCaP and DU145 cell lines were obtained from the American Type Culture Collection. LNCaP cells were grown in RPMI 1640 supplemented with 10% fetal bovine serum without antibiotics. DU145 cells were grown in MEM supplemented with 10% fetal bovine serum without antibiotics. At 24 to 48 h after plating when cells were 50% to 60% confluence, the medium was changed before starting the treatment with PGG or the other agents. To standardize all PGG/drug exposure conditions, cells were bathed in culture medium at a volume to surface area ratio of 0.2 mL/cm^2 (e.g., 15 mL for a T75 flask and 5 mL for a T25 flask). For the experiments in which caspase inhibitor was used, the inhibitor and PGG were given to the cells at the same time. For the experiment in which antioxidants were used, the cells were exposed to *N*-acetyl-L-cysteine or manganese(III) tetrakis(*N*-methyl-2-pyridyl)porphyrin for 2 h before initiating treatment with PGG. DMSO (≤2 μL/mL) was added as a vehicle solvent to the control culture that did not receive the inhibitor. This concentration of DMSO did not cause any adverse morphologic response.

Crystal Violet Staining

For the evaluation of overall inhibitory effect of PGG on cell number, the cells were treated with PGG daily for 4 days. After treatment, the culture medium was removed and the cells were fixed in 1% glutaraldehyde solution in PBS for 15 min. The fixed cells were stained with 0.02% aqueous solution of crystal violet for 30 min. After washing with PBS, the stained cells were solubilized with 70% ethanol. The absorbance at 570 nm with the reference filter 405 nm was evaluated using a microplate reader (Beckman Coulter).

Apoptosis Evaluation

Apoptosis was assessed by multiple methods. The first was a cell death detection ELISA kit purchased from Roche Diagnostics. The second was Annexin V staining of externalized phosphatidylserine in apoptotic cells by flow cytometry using Annexin V/FITC Staining Kit from MBL International. The third method was immunoblot analysis of PARP cleavage. All these methods were as described previously (28, 29).

Immunoblot Analyses

The cell lysate was prepared in ice-cold radioimmunoprecipitation assay buffer as described previously (28). Immunoblot analyses were essentially as described (28), except that the signals were detected by enhanced chemofluorescence with a Storm 840 scanner (Molecular Dynamics).

RNA Interference

The siRNAs for human p53, p21, or Bak were purchased from Santa Cruz Biotechnologies. The cells were transfected with 20 nmol/L siRNAs using INTERFERin transfection reagent (Polyplus Transfection) for 24 h and then were used for subsequent experiments with PGG treatment.

Analysis of Reactive Oxygen Species

Generation of intercellular reactive oxygen species (ROS) was measured by flow cytometry following staining with hydroethidine and 6-carboxy-2′,7′-dichlorodihydrofluorescein diacetate, which have been shown to specifically detect superoxide and hydrogen peroxide (30, 31), as we have recently described (32, 33). The hydroethidine is a reduced form of ethidium. Upon oxidation by superoxide, red fluorescent ethidium accumulates in the nucleus. 6-Carboxy-2′,7′-dichlorodihydrofluorescein diacetate is a reduced form of 2,7-dichlorofluorescein. Oxidation by hydrogen peroxide can be detected by monitoring the increase in green fluorescence with a flow cytometer. At 30 min before harvest, hydroethidine and 6-carboxy-2′,7′-dichlorodihydrofluorescein diacetate were added to the medium to a concentration of 2 and 5 μmol/L, respectively. The cells were collected as described above, and the ethidium and 2,7-dichlorofluorescein fluorescence was measured using a Becton Dickinson flow cytometer.

Table 1. Cell cycle distribution

	PGG 50 μmol/L exposure duration							
	6 h		12 h		24 h		48 h	
	Control	+PGG	Control	+PGG	Control	+PGG	Control	+PGG
LNCaP								
G_1	76	83	72	85	70	83	79	76
S	13	13	18	13	20	15	10	24
G_2	11	3	10	3	10	2	11	0
DU145								
G_1	48	63	53	67	54	62	62	51
S	32	27	27	26	32	36	25	42
G_2	20	10	19	6	13	3	13	7

NOTE: These patterns are representative of two to three experiments in each cell line; DMSO as control.

Animal Study

The animal use protocol was approved by the Institutional Animal Care and Use Committee of the University of Minnesota, and carried out at The Hormel Institute's Animal Facility. PGG was given daily by i.p. injection (20 mg/kg body weight) starting 7 days before s.c. inoculation of cancer cells (''prevention'' setting) for 45 days. This dose was chosen based on earlier work with LLC allograft (26). To establish cancer xenograft, 2×10^6 DU145 cells were mixed with Matrigel (50%) (Becton Dickinson) and injected s.c. into the right flank of 7- to 8-week-old male BALB/c athymic nude mice (NxGen BioSciences). Tumors were measured twice per week with a caliper and tumor volumes were calculated using the following formula: $1 / 2 (w_1 * w_2 * w_2)$, where w_1 is the largest tumor diameter and w_2 is the smallest tumor diameter.

Immunohistochemistry

Immunostaining for pSTAT3 Tyr^{705} was done with an antibody from Cell Signaling Technology. Antigen retrieval was done after deparaffinization and rehydration of the tissue sections (4 μm) by microwave for 10 min in 1 mmol/L EDTA. Sections were cooled to room temperature, treated with 3% hydrogen peroxide in methanol for 10 min, and blocked with 6% horse serum for 40 min at room temperature. Sections were then incubated with the primary antibody to phospho-STAT3 (diluted 1:150; Cell Signaling Technology) at 4°C overnight. Sections were washed in PBS and incubated with the secondary antibody (biotinylated goat anti-rabbit; 1:150; Vector Laboratories) for 30 min. After further washes, color was developed by indirect avidin/biotin-enhanced horseradish peroxidase method with the DAKOCytomation ABCcomplex/Horseradish Peroxidase kit and with 3,3′-diaminobenzidine tetrahydrochloride as substrate.

For semiquantitation, 10 representative ×200 power photomicrographs were taken with a digital camera, avoiding gross necrotic areas. The positively stained cancer epithelial cells within each photomicrograph were counted. The counting of total cancer cells was aided with the ImagePro+ image processing program.

Statistical Analyses

Numerical data were expressed as mean ± SE. Statistical analyses were carried out with Prism and Sigma plot softwares, and $P < 0.05$ was considered statistically significant. The data were analyzed by ANOVA followed by Bonferroni t test for pairwise multiple comparisons or other appropriate tests. When only two groups were in an experiment, Student's t test was used.

Results

PGG Inhibited Growth of Prostate Cancer Cells of Different p53 and Androgen Dependence Status

To assess the direct inhibitory effect of PGG on prostate cancer cells, we exposed sparsely seeded LNCaP (p53 wild-type, androgen-dependent) and DU145 (mutant p53, androgen independent) cells to daily changes of fresh medium containing PGG (25-75 μmol/L) for 4 days. This schedule simulates a pill-a-day regimen. As shown in Fig. 1A, PGG exerted a strong dose-dependent inhibitory effect on both cell lines. In PC-3 cells (p53-null and androgen-independent), the growth-inhibitory efficacy was identical to DU145 cells (data not shown). These data therefore indicated that PGG inhibited prostate cancer cell growth regardless of their p53 status and androgen dependence status.

PGG Induced G_1 and S Cell Cycle Arrests

To determine whether cell cycle arrests contributed to the growth-inhibitory action of PGG, we analyzed LNCaP and DU145 cells treated with PGG for different duration by flow cytometry (Table 1). We observed a rapid enrichment of G_1 cells at the expense of G_2 cells in LNCaP and DU145 cell lines from 6 to 12 h exposure to 50 μmol/L PGG (Table 1). However, from 24 to 48 h, cells accumulated in the S phase, with near elimination of G_2 cells (Table 1). In PC-3 cells, the same patterns of cell cycle arrests were observed (data not shown). These data indicated that PGG inhibited cell proliferation by arresting cells not only in G_1 phase but also in S phase.

PGG Induced Caspase-Mediated Apoptosis in LNCaP and DU145 Cells

In addition to cell cycle arrests, morphologic observations of PGG-treated DU145 and LNCaP cancer cells suggested that an induction of cell death contributed to the overall growth inhibition. To determine whether cell death induced by PGG involved caspase activation, we analyzed cleavage of PARP using Western blot (Fig. 1B). In LNCaP cells, caspase-mediated cleavage of PARP was time dependent (detected as early as 12 h) and was PGG concentration dependent (48 h time point). Because PGG has been reported to suppress PSA secretion into the conditioned medium of LNCaP cells (22), we analyzed the abundance of PSA and androgen receptor proteins in the cell lysate of PGG-treated LNCaP cells (Fig. 1B). We detected a decrease of androgen receptor and PSA expression at 24 h of PGG treatment. By 48 h, a PGG

concentration-dependent decrease of both proteins was observed, but the effects were not dissociable from apoptosis as indicated by cleaved PARP. Therefore, the reported effect of PGG on androgen receptor and PSA (22) was likely secondary to cell death.

The PARP cleavage in LNCaP cells was accompanied by the cleavage activation of the executioner caspase-3 (19-kDa active forms) and the apical caspases of the mitochondria pathway (caspase-9, 37-kDa active form) and death receptor pathway (caspase-8, 43/41-kDa cleavage intermediates; Fig. 1B). In DU145 cells (Fig. 1C), PARP cleavage was delayed in comparison with LNCaP cells. By 48 h of PGG treatment, cleavage of caspase-3, -9, and -8 were detected in a PGG concentration-dependent manner. The results indicated that caspase activation through both intrinsic and extrinsic cascades was involved in PGG-induced apoptosis in these two cell lines, although the time kinetics showed slower activation in DU145 cells than in LNCaP cells.

To test whether caspase activation was critical for cell death induced by PGG in both cell lines, we assessed the effect of a pan-caspase inhibitor on PGG-induced cell death measured by a cell death ELISA kit for oligonucleosomes in the apoptotic cells. As shown in Fig. 1D, 40 μmol/L pan-caspase inhibitor completely blocked PGG-induced cell death in both DU145 and LNCaP cells. This conclusion was further confirmed by Annexin V staining assay (data not shown). Taken together, PGG induced predominantly caspase-mediated apoptosis in LNCaP (p53 wild-type and androgen-dependent) and DU145 (mutant p53, androgen-independent) prostate cancer cells.

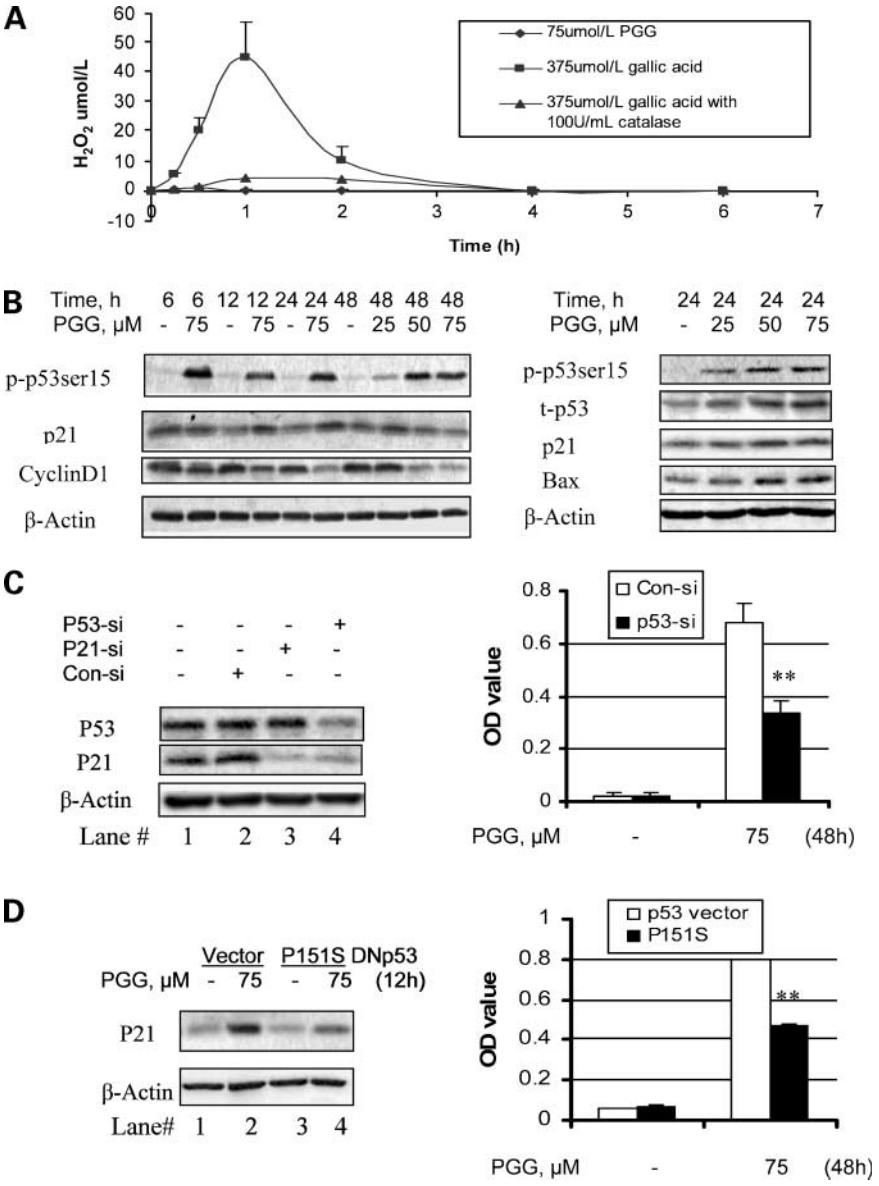

Figure 2. PGG induces p53-mediated apoptosis in LNCaP prostate cancer cells without cell-free hydrogen peroxide generation. **A,** lack of H_2O_2 generation in cell-free culture medium by PGG. PGG or gallic acid (equal concentration of phenol groups) were added to MEM with or without 10% fetal bovine serum are maintained in a humidified incubator at 37°C in a 5% CO_2 environment. At different time points, measurement of the concentration of H_2O_2 in the medium was done as described by Nakagawa et al. (34). Catalase effectively quenched gallic acid – induced H_2O_2. **B,** Western blot analysis of PGG-treated LNCaP cells for p53 Ser^{15}, $p21^{Cip1}$, Bax, and cyclin D1. **C,** effect of knocking down of p53 on PGG-induced apoptosis in LNCaP cells. Efficiency of p53 knockdown by siRNA was verified by Western blot (*left*) at 24 h post-transfection with 20 nmol/L p53 siRNA using INTERFERin. Apoptosis (*graph, right*) was estimated by Cell Death ELISA when the siRNA-transfected LNCaP cells were treated with 75 μmol/L for 48 h. **, $P < 0.01$, compared with control siRNA ($n = 4$). **D,** effect of dominant-negative p53 on PGG-induced apoptosis. Inhibition of PGG-induced p53 transcriptional activity in DN-P151S cells (generously provided by Ralph W. deVere White, Department of Urology, University of California) was evident by the attenuation of $p21^{Cip1}$ induction (*left*). Apoptosis (*graph, right*) was estimated by Cell Death ELISA in vector and dominant-negative p53 cells after exposure to 75 μmol/L for 48 h. **, $P < 0.01$ compared with vector control ($n = 4$).

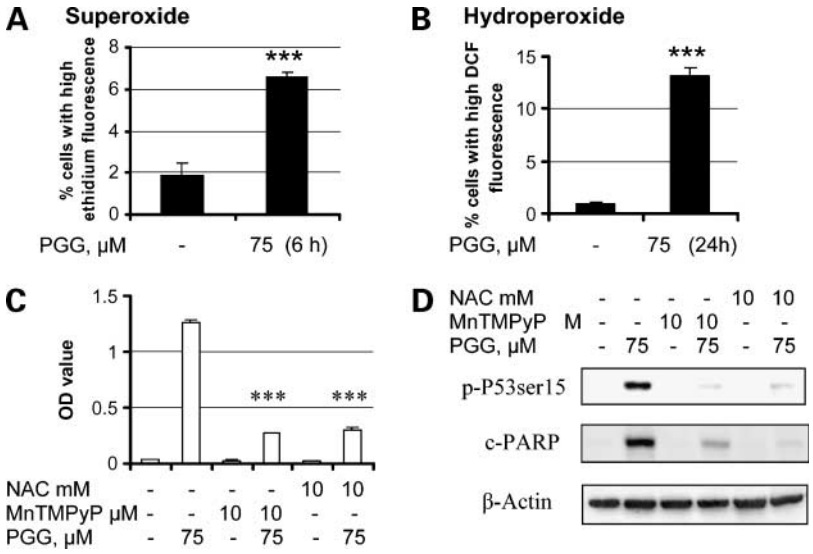

Figure 3. Intracellular ROS generation by PGG triggers p53 activation. **A,** percentage of cells with high ethidium fluorescence after 6 h treatment in LNCaP cells. ***, $P < 0.001$, compared with control ($n = 4$). **B,** percentage of cells with high 2,7-dichlorofluorescein fluorescence after 24 h treatment in LNCaP cells. ***, $P < 0.001$, compared with control ($n = 4$). **C,** effects of antioxidants on PGG-induced apoptosis in LNCaP cells. The cells were pretreated with either 10 μmol/L manganese(III) tetrakis(*N*-methyl-2-pyridyl)porphyrin or 10 mmol/L *N*-acetyl-L-cysteine for 2 h and then exposed to 75 μmol/L PGG for 48 h. Apoptosis was measured by Cell Death ELISA. ***, $P < 0.001$, compared with PGG treatment alone ($n = 4$). **D,** Western blot detection of effects of antioxidants on PGG-induced p53 Ser^{15} phosphorylation and PARP cleavage. The cells were treated identically as in **C**, except exposure to 75 μmol/L PGG for 24 h.

PGG Did Not Induce Cell-Free Production of Hydrogen Peroxide

It has been shown that the cytotoxic effects of some polyphenolic compounds such as gallic acid and green tea polyphenol epigallocatechin-3-gallate are due to hydrogen peroxide generated by these compounds in the culture medium (34–36). Because PGG is a glucose ester of five gallic acid molecules, we compared the production of hydrogen peroxide in the cell-free medium by PGG with gallic acid in equal molar concentration of phenol groups. As shown in Fig. 2A, gallic acid induced a significant production of hydrogen peroxide, peaking at 1 h (*squares*), which was quenched by catalase added to the cell culture medium (*triangles*). PGG did not induce cell-free hydrogen peroxide production within the time frame shown (Fig. 2A) and throughout 24 h (data not shown). These data support PGG as a distinct entity from gallic acid or epigallocatechin-3-gallate to induce cell cycle G_1 and S arrests (Table 1) and caspase-mediated apoptosis. Indeed, it has been reported that, in DU145 cells, gallic acid induces S-phase arrest (6-12 h), progressing to G_2-M arrest (24 h) with associated changes in DNA damage response/ATM activation and checkpoint kinase Chk2 activation (37).

PGG-Induced Apoptosis in LNCaP Cells Was Principally p53 Mediated

In LNCaP cells, as in many other cell types, sustained activation of p53 is often associated with caspase-mediated apoptosis (38). We examined whether the observed apoptosis effect of PGG in LNCaP cells was accompanied by an activation of this pathway. As shown in Fig. 2B (*left*), PGG induced a rapid and persistent p53 Ser^{15} phosphorylation in LNCaP cells, some 6 h ahead of the up-regulation of $p21^{Cip1}$ protein, which is the best known transcriptional target of p53 (39). PGG also decreased the abundance of cyclin D1 as early as 6 h of exposure and persisted through 48 h, suggesting a possible mechanism for G_1 arrest due to a consequential decrease of CDK4/CDK6 activities to drive G_1 cell cycle progression. Activation of p53 through Ser^{15} phosphorylation by PGG correlated with the induction of not only $p21^{Cip1}$ but also Bax, which is another known transcriptional target of p53 (40), in a PGG concentration-dependent manner at 24 h of treatment (Fig. 2B, *right*). These results indicated that the transcriptional activity of p53 was enhanced by PGG treatment.

To determine the role of p53 activation in PGG-induced apoptosis in LNCaP cells, we tested the effect of attenuating p53 by siRNA. As shown in Fig. 2C (*left*), p53 siRNA caused a significant reduction of p53 protein expression, which correlated with an inhibition of $p21^{Cip1}$ (*lane 4* versus *lane 2*) and the specificity of $p21^{Cip1}$ down-regulation was verified by p21 siRNA (*lane 3*). Knocking down of p53 by siRNA led to a >50% decrease of PGG-induced apoptosis in LNCaP cells (Fig. 2C, *graph*). The role of p53 in PGG-induced apoptosis was further tested by an ectopic expression of a dominant-negative mutant p53 DN-P151S (32, 41). The inhibition of p53 transcriptional function by dominant-negative mutant was evident by the reduced $p21^{Cip1}$ induction with PGG treatment (Fig. 2D, *left, lane 4* versus *lane 2*). The attenuation of p53 activation led to a 45% reduction of PGG-induced apoptosis in DN-P151S cells compared with that in vector control cells (Fig. 2D, *graph*). The results from both types of genetic manipulation supported a major (but not sole) mediator role for p53 in caspase-mediated apoptosis by PGG in LNCaP cells.

Intracellular ROS Generation Mediated p53 Activation and Apoptosis in LNCaP Cells

We hypothesized that the activation of p53 and caspase-mediated apoptosis by PGG in LNCaP cells might involve ROS generation. We measured intracellular ROS by flow cytometry following 2′,7′-dichlorofluorescein (preferentially detecting hydroperoxide) and DHE (preferentially detecting superoxide) staining as described in Materials and Methods. A significant increase of DHE-positive cells was observed at 6 h in LNCaP cells after PGG treatment (Fig. 3A) followed by a strong increase of 2′,7′-dichlorofluorescein-positive cells at 24 h (Fig. 3B).

We tested the effects of two antioxidants on apoptosis induction by PGG (Fig. 3C). The apoptosis induction by PGG was significantly reduced by either manganese(III) tetrakis(*N*-methyl-2-pyridyl)porphyrin, a cell-permeable superoxide dismutase mimetic, or *N*-acetyl-L-cysteine, a precursor of intracellular glutathione synthesis and ROS scavenger. Attenuation of ROS production by either manganese(III) tetrakis(*N*-methyl-2-pyridyl)porphyrin or *N*-acetyl-L-cysteine significantly decreased PGG-induced p53 Ser^{15} phosphorylation and PARP cleavage (>90%; Fig. 3D). Taken together, the results support a critical role of intracellular ROS generation in PGG-induced p53 activation and caspase-mediated apoptosis in LNCaP cells.

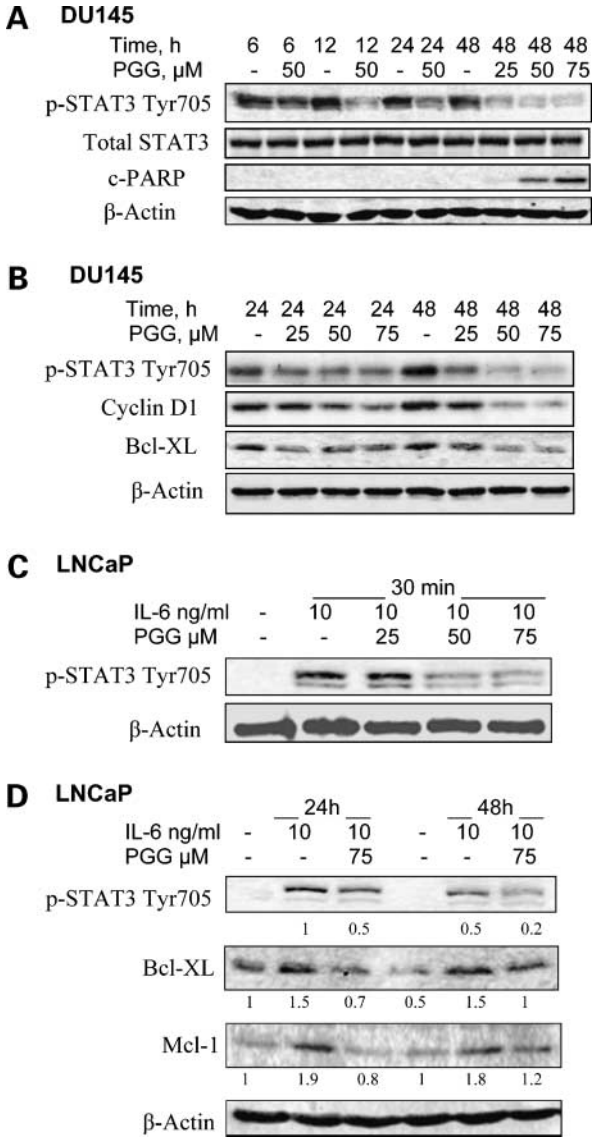

Figure 4. PGG inhibits constitutive and IL-6-induced STAT3 activation in prostate cancer cells. **A,** Western blot analyses of time course of PGG-induced inhibition of STAT3 Tyr^{705} phosphorylation in DU145 cells in relationship to PARP cleavage. **B,** Western blot analyses of the dose response of PGG-induced inhibition of STAT3 Tyr^{705} phosphorylation and its downstream targets cyclin D1 and Bcl-XL in DU145 cells. **C,** Western blot analyses of the dose response of PGG-induced inhibition of IL-6-induced STAT3 Tyr^{705} phosphorylation in LNCaP cells. **D,** Western blot analyses of the PGG-induced inhibition of IL-6-induced STAT3 Tyr^{705} phosphorylation and its transcriptional targets Bcl-XL and Mcl-1 in LNCaP cells.

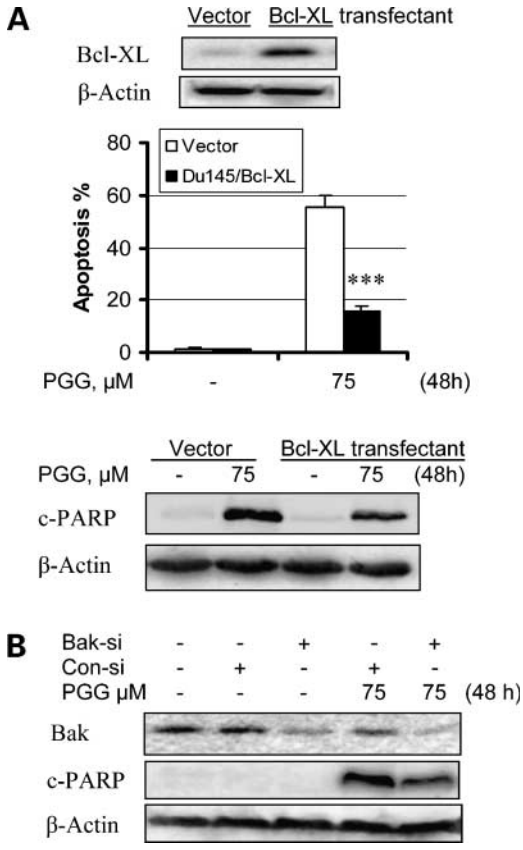

Figure 5. Overexpression of Bcl-XL or knockdown of Bak attenuates PGG-induced cell death in DU145 cells. **A,** Western blot verification of Bcl-XL expression in Bcl-XL-overexpressing DU145 cells versus vector control cells (generously provided by Prof. Peter Daniel, Humboldt University). Apoptosis was quantified by Annexin V staining and Western blot of cleaved PARP. ***, $P < 0.001$ ($n = 4$). **B,** knockdown of Bak by siRNA in DU145 cells was verified by Western blot. Apoptosis was detected by PARP cleavage.

PGG Inhibited Constitutive and IL-6-Induced STAT3 Activation in Prostate Cancer Cells

Because DU145 cells contain nonfunctional mutant p53 (42), PGG must induce caspase-mediated apoptosis also through p53-independent targets and pathways. To test whether STAT3 might be targeted by PGG in DU145 cells, we analyzed the effect of PGG on STAT3 phosphorylation status (Fig. 4A). PGG treatment caused a rapid (as early as 6 h) and persistent (throughout 48 h) inhibition of STAT3 Tyr^{705} phosphorylation, ahead of PARP cleavage by >24 h (Fig. 4A). Furthermore, inhibition of phospho-STAT3 by PGG dose-dependently correlated with a reduction of Bcl-XL, a key mitochondria protective protein of the Bcl-2 family and of cyclin D1, both being transcriptional targets of STAT3 (ref. 14; Fig. 4B).

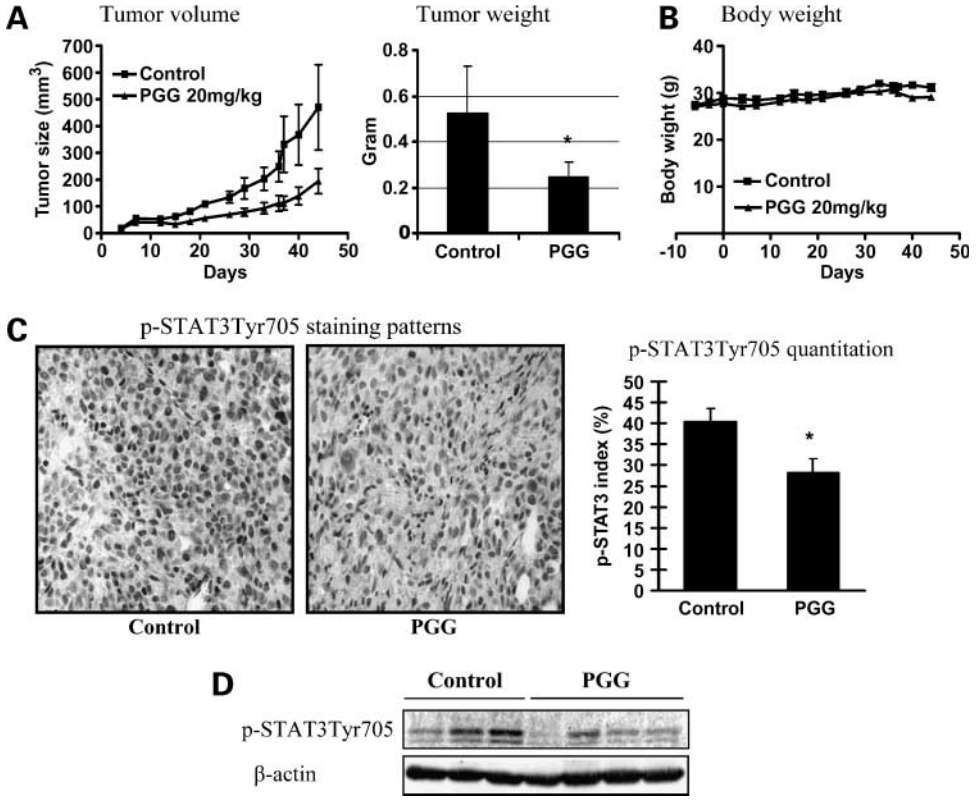

Figure 6. PGG inhibits DU145 xenograft tumor growth and STAT3 Tyr^{705} phosphorylation *in vivo*. **A,** tumor growth kinetics and final tumor weight after necropsy. PGG (20 mg/kg) was given daily by i.p. injection 7 d before cancer cell inoculation by s.c. injection ($n = 16$ mice per group). Final tumor weight at termination of experiment 45 d after tumor inoculation. *, $P < 0.05$, compared with control group. **B,** Body weight of mice at termination of experiment. There was no statistical difference between PGG-treated and control group. **C,** immunohistochemical staining for phospho-STAT3 Tyr^{705} (*brown*) and counterstained with Mayer's hematoxylin solution (*blue*). Magnification, ×200. *Columns,* mean; *bars,* SE ($n = 10$ selected tumors). *, $P < 0.05$, compared with control group. **D,** Western blot analysis of phospho-STAT3 Tyr^{705} in selected xenograft tumors.

Whereas most articles have reported that LNCaP cells do not contain constitutively active STAT3 (43, 44), some have reported the contrary (e.g., ref. 16). Presumably, such discrepancy is due to variations in cell passage status and culture conditions among different laboratories. We did not observe phosphorylation of STAT3 in LNCaP cells under conditions where DU145 cells showed strong STAT3 Tyr^{705} phosphorylation (data not shown). We therefore tested whether IL-6-induced STAT3 activation could be inhibited by PGG in LNCaP cells. IL-6 caused a rapid (30 min; Fig. 4C) and persistent (24 and 48 h) STAT3 Tyr^{705} phosphorylation (Fig. 4D) and induction of Bcl-XL and Mcl-1, which are known transcriptional targets of STAT3 (14). Treatment with PGG led to a significant decrease of IL-6-induced STAT3 Tyr^{705} phosphorylation (Fig. 4C and D) and Bcl-XL/Mcl-1 expressions in LNCaP cells (Fig. 4D). These results suggest that PGG was capable of inhibiting both constitutive and IL-6-induced STAT3 Tyr^{705} phosphorylation in prostate cancer cells, contributing to apoptosis signaling and cell cycle arrests.

Overexpression of Bcl-XL or Knockdown of Bak Decreased PGG-Induced Apoptosis in DU145 Cells

To evaluate the functional significance of down-regulation of STAT3-target Bcl-XL in PGG-induced caspase-mediated apoptosis, we tested the effect of an overexpression of Bcl-XL on apoptosis induction by PGG in DU145 cells (Fig. 5A). Apoptosis by PGG in the DU145 cells overexpressing Bcl-XL were decreased by >72% in comparison with the vector control cells (55.7% versus 15.5%). Western blot analysis showed a corresponding decrease of PARP cleavage (Fig. 5A), supporting decreased Bcl-XL contributed critically to PGG-induced caspase-mediated apoptosis in DU145 cells.

Down-regulation of Bcl-XL and Mcl-1 through suppression of STAT3 activity by PGG could be expected to free their binding partners Bak and Bax, which in turn lead to mitochondrial permeability change and the activation of caspases in the intrinsic pathway. We tested the effect of knocking down Bak on PGG-induced apoptosis in DU145 cells, which do not express Bax (Fig. 5B). Knocking down of Bak decreased PGG-induced PARP cleavage by half. These results implicated mitochondria-dependent caspase activation to play a major role in PGG-induced apoptosis.

PGG Inhibited Prostate Tumor Growth *In vivo*

The strong growth-inhibitory effects of PGG against these prostate cancer cells prompted us to evaluate the *in vivo* growth-inhibitory effect of PGG using the DU145 xenograft model. PGG was given by i.p. injection (20 mg/kg body weight) starting 7 days before s.c. inoculation of cancer cells (''prevention'' setting). This dose was chosen based on earlier work with mouse LLC allograft model by coauthor Kim's group (26). As shown in Fig. 6A, treatment with PGG led to a significant inhibition of tumor growth (ANOVA, $P < 0.01$) and decreased the final tumor weight by 53% ($P < 0.05$). The PGG-treated group did not show decreased body weight of the mice (Fig. 6B). Immunohistochemistry staining of excised tumor sections showed strong nuclear localization of

phospho-STAT3 Tyr^{705} (Fig. 6C). The percent nuclei positive for phospho-STAT3 staining was decreased by one third (Fig. 6C). Western blot analyses of selected frozen tumors showed the same trend of decreased phospho-STAT3 abundance in PGG-treated group (Fig. 6D). Overall, the data suggest that *in vivo* targeting of phospho-STAT3 by PGG contributed to its *in vivo* efficacy against DU145 prostate cancer xenograft growth.

Discussion

Given carcinogenesis is a multistage dynamic process involving alterations of numerous oncogenic signaling pathways and inactivation of tumor suppressor pathways (45), the lack of success with single-target approach for treatment and prevention is not surprising. Development of agents that can affect diverse molecular targets and cellular processes is urgently needed to improve prostate cancer chemoprevention and therapy. Here, we have shown that PGG might be one such novel agent that induces caspase-mediated apoptosis as well as G_1- and S-phase arrests in prostate cancer cells of diverse p53 and androgen dependence status. The decreased cyclin D1 in PGG-treated LNCaP cells (Fig. 2A) and DU145 cells (Fig. 4B) could be important to account for the rapid induction of G_1 arrest by PGG through diminished CDK4/CDK6 activity, which requires cyclin D1 (46). The mechanisms responsible for the G_1 and S arrests are currently under investigation.

We provided strong evidence that PGG could activate the p53 tumor suppressor signaling pathway and inhibit the STAT3 oncogenic signaling cascade to induce caspase-mediated apoptosis in prostate cancer cells. In particular, we found that PGG induced a rapid and persistent p53 phosphorylation (Fig. 2), which was temporally hours ahead of PARP cleavage indicative of the activation of caspases (Fig. 1). The genetic approach with either siRNA (Fig. 2C) or dominant-negative mutant (Fig. 2D) to inactivate p53 signaling supports a major role (although not a sole mediator) of p53 activation in PGG-induced apoptosis in LNCaP cells. We identified ROS generation as a major mediator of p53 activation and apoptosis because two antioxidants effectively blocked p53 activation and caspase activation and overall apoptosis (Fig. 3). Taken together, our results support the induction of intracellular ROS by PGG leads to p53 activation, which in turn stimulates Bax and mitochondria-dependent activation of caspases as a predominant apoptosis signaling pathway in LNCaP cells. Apoptosis induction by PGG in LNCaP cells is faster than DU145 cells and may be associated with a rapid p53 phosphorylation.

The growth-inhibitory effect of PGG on LNCaP cells was similar to that on DU145 and PC-3 cells, which do not have functional p53 (42), suggesting that PGG possesses additional targets. We focused on STAT3 for several reasons: (*a*) Janus-activated kinase/STAT3 activation is involved in the development of hormone-refractory prostate cancer by either ligand-independent activation of androgen receptor or through direct transcriptional mechanisms (18, 47, 48). (*b*) DU145 and PC-3 cells are androgen-independent prostate cancer cells with constitutively active STAT3 (16). (*c*) Block of constitutive STAT3 signaling results in growth inhibition and apoptosis of androgen-independent prostate cancer cells *in vitro* and *in vivo* (16, 17), supporting their dependence on and addiction to constitutive STAT3 signaling for growth and survival. In this study, we found that PGG inhibited constitutively active STAT3 in androgen-independent DU145 prostate cancer cells (Fig. 4A), which was correlated with down-regulation of its transcriptionally regulated targets such as Bcl-XL and cyclin D1 (Fig. 4B). Given the important role of IL-6-signaling in STAT3 activation and prostate cancer progression to androgen independence (18, 43), we tested the effect of PGG on IL-6-induced STAT3 activation using LNCaP cells, which do not have constitutively active STAT3. We found that PGG also has the capacity of inhibiting IL-6-induced STAT3 activation and Bcl-XL expression in LNCaP cells (Fig. 4C and D).

To further study the functional role of inactivation of STAT3/Bcl-XL axis in PGG-induced apoptosis, we tested the effect of overexpression of Bcl-XL or knockdown of Bcl-XL binding partner Bak on apoptosis by PGG (Fig. 5). The results of both manipulations support the important role of STAT3/Bcl-XL-mediated mitochondrial activation in PGG-induced apoptosis in DU145 cells. Together, these data show, for the first time, PGG as a potent anti-STAT3 agent that targets both constitutive and IL-6-induced STAT3 activation (Tyr^{705} phosphorylation) in human prostate cancer cell lines. Furthermore, an *in vivo* inhibitory effect of PGG on STAT3 activation was observed in xenograft tumors (Fig. 6C and D). How PGG decreases STAT3 phosphorylation will be investigated in future work.

The xenograft study is, to our knowledge, the first to show the *in vivo* efficacy of PGG against the growth of human prostate cancer cells (Fig. 6A). The data confirmed the *in vivo* efficacy of PGG against the mouse LLC allograft model (26) and extended it by showing that the anti-prostate cancer activity did not require immunocompetence because of the nude mice are severely immunocompromised. In terms of the route of PGG administration, we used i.p. injection to deliver PGG in the current study as in the LLC model (26) for proof of principle. To address the issue of oral bioavailability of PGG, we have in a separate study with the LLC allograft model tested the efficacy of oral gavage of 10 mg PGG/kg body weight starting 12 days after cancer inoculation. We observed a 60% inhibition of tumor weight after 7 days of PGG therapeutic treatment (final tumor weight in g/mouse: vehicle 1.35 ± 0.25 versus PGG 0.55 ± 0.15; $n = 7$ mice; t test, $P < 0.001$). The demonstration of oral efficacy is important for the practical use of PGG as a chemopreventive agent because oral intake is a noninvasive means to deliver PGG to internal target organ sites such as the prostate.

In summary, PGG can activate p53 tumor suppressor and inactivate STAT3 oncogenic signaling to mediate its proapoptotic and antiproliferative effects in prostate cancer cells. These actions may, at least in part, account for the inhibition of human xenograft tumor growth *in vivo*. Taken together, our data strongly suggest that PGG has an excellent potential for prostate cancer chemoprevention or treatment.

Disclosure of Potential Conflicts of Interest

All authors have no personal or financial conflict of interest and have not entered into any agreement that could interfere with our access to the data on the research or on our ability to analyze the data independently, to prepare articles, and to publish them.

Acknowledgments

We thank Prof. Peter Daniel (Humboldt University) for the stable DU145 cell lines transfected with the pIRES-neo-Bcl-xL or the pIRES-neo control plasmid, Prof. Ralph W. deVere White (Department of Urology, University of California) for generously providing the p53 dominant-negative mutant LNCaP cells, Todd Schuster for performing flow cytometry and Annexin V staining, the animal care staff of the Hormel Institute Animal facility for excellent animal care and health monitoring, and Andria Hansen for submission of the article.

References

1. Jemal A, Siegel R, Ward E, et al. Cancer statistics, 2008. CA Cancer J Clin 2008;58:71 – 96.

2. Klein EA. Chemoprevention of prostate cancer. Annu Rev Med 2006; 57:49 – 63.

3. Sarkar FH, Li Y. Cell signaling pathways altered by natural chemopreventive agents. Mutat Res 2004;555:53 – 64.

4. Turkson J, Jove R. STAT proteins: novel molecular targets for cancer drug discovery. Oncogene 2000;19:6613 – 26.

5. Aggarwal BB, Shishodia S. Molecular targets of dietary agents for prevention and therapy of cancer. Biochem Pharmacol 2006;71:1397 – 421.

6. Vogelstein B, Lane D, Levine AJ. Surfing the p53 network. Nature 2000;408:307 – 10.

7. Wang W, El-Deiry WS. Restoration of p53 to limit tumor growth. Curr Opin Oncol 2008;20:90 – 6.

8. Hastak K, Gupta S, Ahmad N, Agarwal MK, Agarwal ML, Mukhtar H. Role of p53 and NF-κB in epigallocatechin-3-gallate-induced apoptosis of LNCaP cells. Oncogene 2003;22:4851 – 9.

9. She QB, Bode AM, Ma WY, Chen NY, Dong Z. Resveratrol-induced activation of p53 and apoptosis is mediated by extracellular-signal-regulated protein kinases and p38 kinase. Cancer Res 2001;61:1604 – 10.

10. Choudhuri T, Pal S, Das T, Sa G. Curcumin selectively induces apoptosis in deregulated cyclin D1-expressed cells at G_2 phase of cell cycle in a p53-dependent manner. J Biol Chem 2005;280:20059 – 68.

11. Zhong Z, Wen Z, Darnell JE, Jr. Stat3: a STAT family member activated by tyrosine phosphorylation in response to epidermal growth factor and interleukin-6. Science 1994;264:95 – 8.

12. Bromberg JF, Wrzeszczynska MH, Devgan G, et al. Stat3 as an oncogene. Cell 1999;98:295 – 303.

13. Wen Z, Zhong Z, Darnell JE, Jr. Maximal activation of transcription by Stat1 and Stat3 requires both tyrosine and serine phosphorylation. Cell 1995;82:241 – 50.

14. Lassmann S, Schuster I, Walch A, et al. STAT3 mRNA and protein expression in colorectal cancer: effects on STAT3-inducible targets linked to cell survival and proliferation. J Clin Pathol 2007;60:173 – 9.

15. Lin J, Tang H, Jin X, Jia G, Hsieh JT. p53 regulates Stat3 phosphorylation and DNA binding activity in human prostate cancer cells expressing constitutively active Stat3. Oncogene 2002;21:3082 – 8.

16. Mora LB, Buettner R, Seigne J, et al. Constitutive activation of Stat3 in human prostate tumors and cell lines: direct inhibition of Stat3 signaling induces apoptosis of prostate cancer cells. Cancer Res 2002; 62:6659 – 66.

17. Barton BE, Murphy TF, Shu P, Huang HF, Meyenhofer M, Barton A. Novel single-stranded oligonucleotides that inhibit signal transducer and activator of transcription 3 induce apoptosis *in vitro* and *in vivo* in prostate cancer cell lines. Mol Cancer Ther 2004;3:1183 – 91.

18. Lee SO, Lou W, Hou M, de Miguel F, Gerber L, Gao AC. Interleukin-6 promotes androgen-independent growth in LNCaP human prostate cancer cells. Clin Cancer Res 2003;9:370 – 6.

19. Spiotto MT, Chung TD. STAT3 mediates IL-6-induced neuroendocrine differentiation in prostate cancer cells. Prostate 2000;42:186 – 95.

20. Pu YS, Hour TC, Chuang SE, Cheng AL, Lai MK, Kuo ML. Interleukin-6 is responsible for drug resistance and anti-apoptotic effects in prostatic cancer cells. Prostate 2004;60:120 – 9.

21. Lambert JD, Yang CS. Cancer chemopreventive activity and bioavailability of tea and tea polyphenols. Mutat Res 2003;523 – 524:201 – 8.

22. Lee HH, Ho CT, Lin JK. Theaflavin-3,3′-digallate and penta-*O*-galloyl-β-D-glucose inhibit rat liver microsomal 5α-reductase activity and the expression of androgen receptor in LNCaP prostate cancer cells. Carcinogenesis 2004;25:1109 – 18.

23. Chen WJ, Chang CY, Lin JK. Induction of G_1 phase arrest in MCF human breast cancer cells by pentagalloylglucose through the down-regulation of CDK4 and CDK2 activities and up-regulation of the CDK inhibitors p27(Kip) and p21(Cip). Biochem Pharmacol 2003;65:1777 – 85.

24. Hua KT, Way TD, Lin JK. Pentagalloylglucose inhibits estrogen receptor α by lysosome-dependent depletion and modulates ErbB/PI3K/Akt pathway in human breast cancer MCF-7 cells. Mol Carcinog 2006;45:551 – 60.

25. Ho LL, Chen WJ, Lin-Shiau SY, Lin JK. Penta-*O*-galloyl-β-D-glucose inhibits the invasion of mouse melanoma by suppressing metalloproteinase-9 through down-regulation of activator protein-1. Eur J Pharmacol 2002;453:149 – 58.

26. Huh JE, Lee EO, Kim MS, et al. Penta-*O*-galloyl-β-D-glucose suppresses tumor growth via inhibition of angiogenesis and stimulation of apoptosis: roles of cyclooxygenase-2 and mitogen-activated protein kinase pathways. Carcinogenesis 2005;26:1436 – 45.

27. Pan MH, Lin-Shiau SY, Ho CT, Lin JH, Lin JK. Suppression of lipopolysaccharide-induced nuclear factor-κB activity by theaflavin-3,3′-digallate from black tea and other polyphenols through down-regulation of IκB kinase activity in macrophages. Biochem Pharmacol 2000;59:357 – 67.

28. Jiang C, Wang Z, Ganther H, Lu J. Caspases as key executors of methyl selenium-induced apoptosis (anoikis) of DU-145 prostate cancer cells. Cancer Res 2001;61:3062 – 70.

29. Hu H, Jiang C, Ip C, Rustum YM, Lu J. Methylseleninic acid potentiates apoptosis induced by chemotherapeutic drugs in androgen-independent prostate cancer cells. Clin Cancer Res 2005;11:2379 – 88.

30. Narayanan PK, Goodwin EH, Lehnert BE. α Particles initiate biological production of superoxide anions and hydrogen peroxide in human cells. Cancer Res 1997;57:3963 – 71.

31. Rothe G, Valet G. Flow cytometric analysis of respiratory burst activity in phagocytes with hydroethidine and 2′,7′-dichlorofluorescin. J Leukoc Biol 1990;47:440 – 8.

32. Hu H, Jiang C, Schuster T, Li GX, Daniel PT, Lu J. Inorganic selenium sensitizes prostate cancer cells to TRAIL-induced apoptosis through superoxide/p53/Bax-mediated activation of mitochondrial pathway. Mol Cancer Ther 2006;5:1873 – 82.

33. Li GX, Hu H, Jiang C, Schuster T, Lu J. Differential involvement of reactive oxygen species in apoptosis induced by two classes of selenium compounds in human prostate cancer cells. Int J Cancer 2007;120: 2034 – 43.

34. Nakagawa H, Hasumi K, Woo JT, Nagai K, Wachi M. Generation of hydrogen peroxide primarily contributes to the induction of Fe(II)-dependent apoptosis in Jurkat cells by (-)-epigallocatechin gallate. Carcinogenesis 2004;25:1567 – 74.

35. Kern M, Fridrich D, Reichert J, et al. Limited stability in cell culture medium and hydrogen peroxide formation affect the growth inhibitory properties of delphinidin and its degradation product gallic acid. Mol Nutr Food Res 2007;51:1163 – 72.

36. Lee KW, Hur HJ, Lee HJ, Lee CY. Antiproliferative effects of dietary phenolic substances and hydrogen peroxide. J Agric Food Chem 2005;53: 1990 – 5.

37. Agarwal C, Tyagi A, Agarwal R. Gallic acid causes inactivating phosphorylation of cdc25A/cdc25C-cdc2 via ATM-Chk2 activation, leading to cell cycle arrest, and induces apoptosis in human prostate carcinoma DU145 cells. Mol Cancer Ther 2006;5:3294 – 302.

38. Haupt S, Berger M, Goldberg Z, Haupt Y. Apoptosis—the p53 network. J Cell Sci 2003;116:4077–85.

39. Dulic V, Kaufmann WK, Wilson SJ, et al. p53-dependent inhibition of cyclin-dependent kinase activities in human fibroblasts during radiation-induced G_1 arrest. Cell 1994;76:1013–23.

40. Miyashita T, Reed JC. Tumor suppressor p53 is a direct transcriptional activator of the human bax gene. Cell 1995;80:293–9.

41. Nesslinger NJ, Shi XB, deVere White RW. Androgen-independent growth of LNCaP prostate cancer cells is mediated by gain-of-function mutant p53. Cancer Res 2003;63:2228–33.

42. van Bokhoven A, Varella-Garcia M, Korch C, et al. Molecular characterization of human prostate carcinoma cell lines. Prostate 2003; 57:205–25.

43. Giri D, Ozen M, Ittmann M. Interleukin-6 is an autocrine growth factor in human prostate cancer. Am J Pathol 2001;159:2159–65.

44. Flowers LO, Subramaniam PS, Johnson HM. A SOCS-1 peptide mimetic inhibits both constitutive and IL-6 induced activation of STAT3 in prostate cancer cells. Oncogene 2005;24:2114–20.

45. Mimeault M, Batra SK. Recent advances on multiple tumorigenic cascades involved in prostatic cancer progression and targeting therapies. Carcinogenesis 2006;27:1–22.

46. Diehl JA. Cycling to cancer with cyclin D1. Cancer Biol Ther 2002;1: 226–31.

47. Chen T, Wang LH, Farrar WL. Interleukin 6 activates androgen receptor-mediated gene expression through a signal transducer and activator of transcription 3-dependent pathway in LNCaP prostate cancer cells. Cancer Res 2000;60:2132–5.

48. Lee SO, Lou W, Johnson CS, Trump DL, Gao AC. Interleukin-6 protects LNCaP cells from apoptosis induced by androgen deprivation through the Stat3 pathway. Prostate 2004;60:178–86.